

Facies and micromorphology of the Neoproterozoic Upper Diamictite Formation in the Democratic Republic of Congo: new evidence of sediment gravity flow

FRANCK R.A. DELPOMDOR^{1,*}, LUC TACK² & ALAIN R. PRÉAT³¹*Illinois State Geological Survey, University of Illinois, Champaign, IL61820, United States; fdelpomd@illinois.edu.*²*Royal Museum for Central Africa, Tervuren, 3080, Belgium; luc.tack@africamuseum.be.*³*Biogeochemistry and Modeling of the Earth System, Université libre de Bruxelles, Brussels, 1050, Belgium; apreat@ulb.ac.be.** *corresponding author*

ABSTRACT. The Upper Diamictite Formation of the West Congo Supergroup is a diamictite-dominated succession variously interpreted as a continental tillite, glaciomarine, and glacially-influenced or non-glacial debris. This paper presents a detailed macro- and microscale analysis of soft-sediment deformation structures in order (1) to resolve the long-standing debate on the genetic origin of the Upper Diamictite Formation, and (2) to constrain the paleoenvironmental conditions during the Marinoan global event. The predominance of ductile and brittle deformations and grain-to-grain compression, considered as evidence of high strain rates and local high stress conditions, indicate that the diamictites were deposited as mass flows. The presence of probable pelagic clays, limestones, and the absence of direct ice-contact deposits point to a subaqueous gravity flow origin. These diamictites were deposited along the margin or at the foot of the basin slope. They were probably triggered by oversteepening and/or tectonic shocks in the Araçuaí-West Congo Orogen between 630 and 660 Ma. The Upper Diamictite Formation provides no support for the postulated global Marinoan glaciation at this time and underscores the importance of a local tectonic control on the sedimentation.

KEYWORDS: Neoproterozoic, soft-sediment deformation microstructures, sediment gravity flow, tectonics, Lower Congo region.

1. Introduction

Since over a decade, numerous studies have postulated that extremely low global temperatures (-50 °C) existed during successive separate glaciations in the Cryogenian period (770–580 Ma). This would explain not only the presence of ice at sea level near the equator, but also an icy cover on all oceans (Snowball Earth Hypothesis; Kirschvink, 1992; Hoffman et al., 1998; Hoffman & Schrag, 2002). The original suggestion of a “global” glaciation in the Neoproterozoic by Harland (1964) was partly based on paleomagnetic data (Harland & Bidgood, 1959) pointing to low paleolatitudes for these glacial deposits. The latter, widely distributed on all continents, are sharply overlain by a cap carbonate unit, interpreted as the result of a sudden switch back to a greenhouse climate related to the increase of atmospheric carbon dioxide due to volcanic degassing (Hoffman & Schrag, 2002). Despite the absence of many typical “glacial” features (e.g., faceted and striated clasts, dropstones, etc.), most Neoproterozoic diamictites were considered as glacial or periglacial deposits. However, not all reported Neoproterozoic diamictites were interpreted in this way, but also as the result of syntectonic sediment gravity flows (Eyles & Januszczak, 2004, 2007) associated with widespread rifting of the Rodinia Supercontinent.

In this paper, we present a new macro- and microscale structural analysis of the Upper Diamictite Formation (UDF) in the West Congo Supergroup (WCS) of the Democratic Republic of Congo (DRC). This study highlights the non-glaciogenic but rather tectonic-controlled origin of the UDF – previously generally ascribed to the Marinoan global event – and provides constraints on models developed on the African side of the “Adamastor” Basin, which separated the São Francisco and Congo cratons.

2. Regional context

The research area encompasses some 1400 km of exposures along the western margin of the Congo Craton extending from southwestern Gabon, across the Republic of Congo (RC) to the western part of the DRC and to northern Angola (Fig. 1). The Pan-African West Congo Belt (WCB) is part of the Araçuaí-West Congo Orogen (AWCO) formed during Gondwana amalgamation (~550 Ma) (Pedrosa-Soares et al., 2008), and is subdivided into the aulacogen foreland and thrust-and-fold belt domains, that differ in deformation style and metamorphic grade (Tack et al., 2001, 2016). The foreland domain is composed of subtabular unmetamorphosed rocks

and reaches its maximum width of approximately 300 km around 5°S in the Lower Congo region. Correspondingly, it is the reference area for the description of sedimentary strata of the belt (e.g., Frimmel et al., 2006). To the west, in contrast, series of the thrust-and-fold belt domain are metamorphosed (Frimmel et al., 2006). In the DRC, the lithostratigraphic terminology of the WCS has been recently redefined. It is subdivided, from oldest to youngest, into the sedimentary and/or magmatic ~1000–930 Ma Matadi and the ~920–910 Ma Tshela/Seke Banza (including the Inga/Lufu- and Gangila-type bimodal magmatism) and the predominantly sedimentary ~910–560 Ma Cataractes groups (Baudet et al., 2013) (Fig. 2). Correlation of the new and previous terminology (respectively Zadinian, Mayumbian and West Congolian groups) falls out of the scope of this paper but is briefly discussed in Kant-Kabalu et al. (2016). The rocks collectively record a long-lived initial rift episode followed by a passive margin system with carbonate platform deposits. The Cataractes Group (CG) is informally subdivided into the Sansikwa, Haut-Shiloango, Lukala and Mpioka subgroups (Kant-Kabalu et al., 2016) (Fig. 2). Two poorly-sorted diamictites, i.e., the Lower Diamictite Formation (LDF) and the Upper Diamictite Formation (UDF) (Fig. 2) form the upper parts of respectively the Sansikwa and Haut-Shiloango subgroups. Both formations have been interpreted as glaciogenic tillite (Cahen, 1948, 1950, 1963, 1978; Lepersonne, 1951; Kröner & Correia, 1973; Cahen & Lepersonne, 1976) or as submarine mudflow deposits (Schermerhorn & Stanton, 1963; Wagner & Wilhelm, 1971; Schermerhorn, 1981; Vellutini & Vicat, 1983). Recently, the UDF was re-interpreted as sediment gravity flows with possible but only limited glaciogenic influence (Tack et al., 2006; Delpomdor et al., 2016). For the LDF of the WCB, recent sedimentological observations indicate gravity mass deposit characteristics (Muanza-Kant et al., 2016).

3. Geochronology

The absolute age of the WCB is relatively well constrained (Fig. 2). The Sansikwa Subgroup is younger than 920-910 Ma (Tack et al., 2001). Basalts with tholeiitic affinity – including the Kimbundu pillows and hyaloclastic breccias – are interlayered in the LDF whereas the Sansikwa Subgroup is intruded by the Sumbi-type dolerite feeder sills and dykes (De Paepe et al., 1975; Kampunzu et al., 1991). One U-Pb age on baddeleyite single-grains from a dolerite sill yielded a crystallization age of 694 ± 4 Ma (Straathof, 2011), a

younger age than the formerly accepted Sturtian age. In Gabon, zircons of an isolated occurrence of a tuffaceous rock from the metasedimentary Louila Formation (to be correlated with the Haut-Shiloango Subgroup of the DRC) yielded a U-Pb SHRIMP age of $<713 \pm 49$ Ma (Thiéblemont et al., 2009a, 2009b). Both macroscopic and microscopic re-examination of the dated sample (Tack, L., Royal Museum for Central Africa, pers. comm.) showed that, in fact, it is reminiscent of clast-poor facies of the underlying LDF, as described in De Paepé et al. (1975). Because these LDF facies are not readily distinguishable from siliciclastic rocks from the Louila Formation, it is suggested that the 713 Ma age may well apply to the LDF rather than to the Louila Formation. Detrital zircon geochronology and provenance analysis of the LDF gave a maximum depositional age of ~ 700 Ma (Muanza-

Kant et al., 2016). These obtained ages on the LDF constrain the episodic extensional activity recorded on the present-day African side of the AWCO (loosely dated 735–675 Ma “E6” rifting event; Pedrosa-Soares & Alkmin, 2011). Detrital U-Pb single-zircon dating of the bottom contact of the upper formation of the Haut-Shiloango Subgroup (Sh6) points to a probably most reliable maximum depositional age of ~ 650 Ma (Frimmel et al., 2006). Carbonates of the uppermost Haut-Shiloango Subgroup (Sh8) were dated at ~ 645 Ma by near-primary $^{87}\text{Sr}/^{86}\text{Sr}$ ratios (Frimmel et al., 2006; Poidevin, 2007). Two samples of the equivalent Louila Formation only gave a major 900–1100 Ma peak (Affaton et al., 2016), which is thus not relevant in terms of constraining the depositional age of this formation. Detrital U-Pb single-zircon grains from the overlying UDF yielded a maximum age of $<707 \pm 23$ Ma

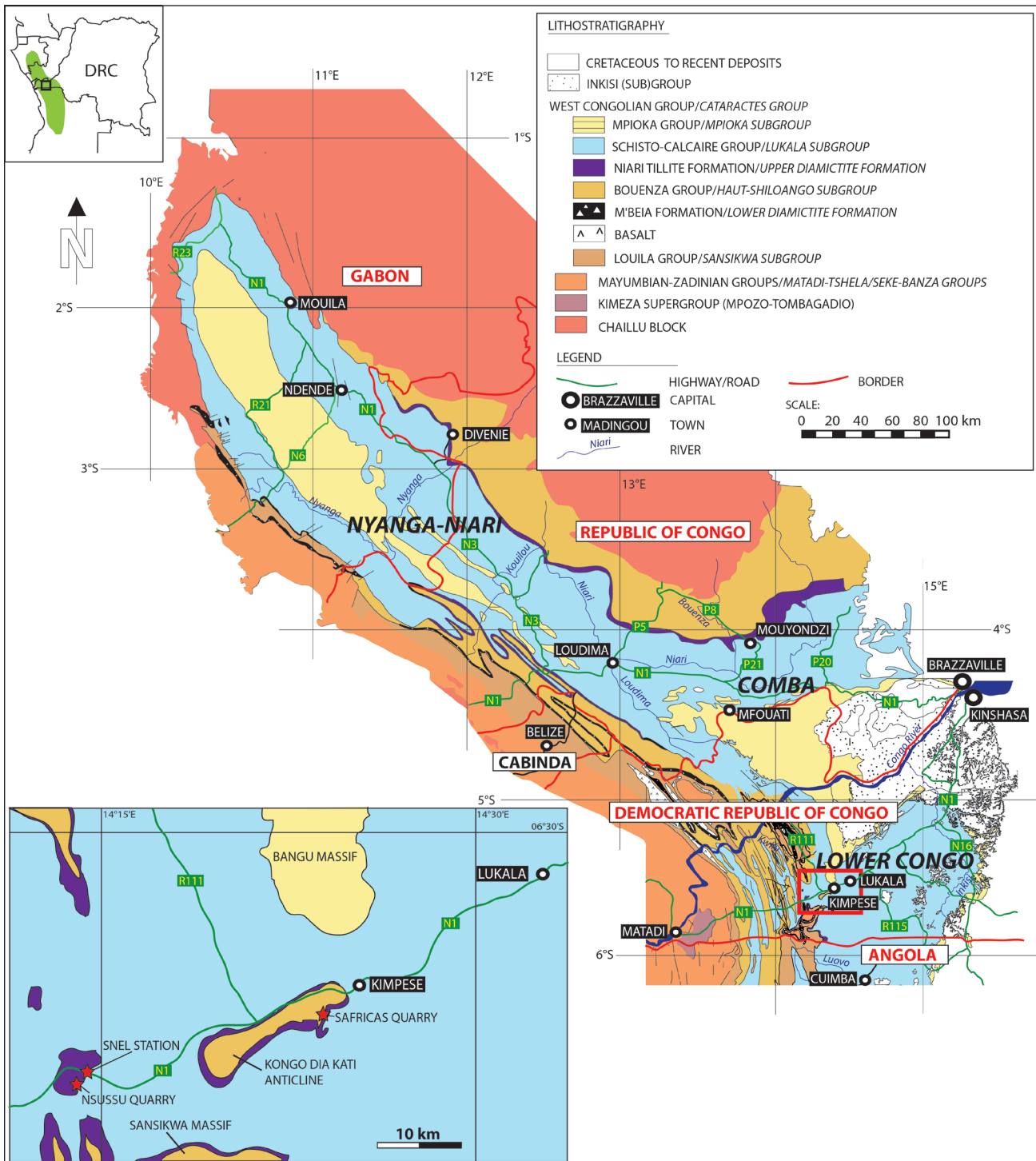


Figure 1. Regional geological map of the West Congo Belt and regional geographic repartition of the Upper Diamictite Formation (modified after Dadet, 1969). Location of studied outcrops (red stars) in the Lower Congo region from the Democratic Republic of Congo (modified after Lepersonne, 1973).

LITOSTRATIGRAPHY		AGE	TECTONIC EVENT
INKISI (SUPER)GROUP		<558 ± 29 Ma	
MPIOKA SUBGROUP		566 ± 42 Ma	ARAÇUAÍ-WEST CONGO OROGEN
LUKALA SUBGROUP (SCHISTO-CALCAIRE SUBGROUP)		<607 ± 16 Ma	
UPPER DIAMICTITE FORMATION		<707 ± 23 Ma	E7 ADAMASTOR OCEAN CLOSURE OF THE
HAUT-SHILOANGO SUBGROUP		<547 ± 45 Ma ~645 Ma ~650 Ma	
LOWER DIAMICTITE FORMATION		<694 ± 4 Ma <700 Ma (<713 ± 49 Ma)	E6 MACAÚBAS RIFTING
SANSIKWA SUBGROUP		<923 ± 43 Ma 912 ± 7 Ma	OPENING OF THE ADAMASTOR OCEAN
TSHELA/SEKE-BANZA & MATADI GROUPS (MAYUMBIAN & ZADINIAN GROUPS)		999 ± 7 Ma	E5 RIFTING BREAKUP OF RODINIA
KIMEZA SUPERGROUP			

AGE: U-Pb (in red), ²⁰⁷Pb-²⁰⁶Pb (in green), ⁴⁰Ar-³⁹Ar (in blue), ⁸⁷Sr/⁸⁶Sr (in purple)

MAGMATIC EVENT:

-  TYPE-? (~630 Ma)
-  TYPE-KIMBUNGU AND -SUMBI (~700 Ma)
-  TYPE-GANGILA AND -SHINKAKASA (930-870 Ma)
-  TYPE-NOQUI (1.0 Ga)

Figure 2. Updated lithostratigraphic subdivisions coupled with geochronology of the West Congo Supergroup in the Lower Congo region (modified after Kant-Kabalu et al., 2016) in combination with tectono-magmatic and orogenic events defined by Pedrosa-Soares & Alkmin (2011). The former stratigraphic terminology is added in parenthesis.

(Straathof, 2011) and a small peak of 600-800 Ma (Affaton et al., 2016). Carbonates of the Schisto-Calcaire Subgroup (C4) – overlying the UDF – were dated at ~575 Ma by near-primary ⁸⁷Sr/⁸⁶Sr ratios (Poidevin, 2007). A <607 ± 16 Ma maximum age of detrital zircons for the Mpiooka Subgroup is given by Straathof (2011) whereas 500–800 Ma peaks for detrital zircon dating are given by Affaton et al. (2016). Regional metamorphism of the WCB gave an Ar-Ar age of 566 Ma (Fig. 2; Frimmel et al., 2006), in good agreement with the ~585–560 Ma orogenic climax of the AWCO in Brazil (Pedrosa-Soares et al., 2011).

4. Materials and methods

Three sections, exposed along N1 Highway about 200 km southwestern of Kinshasa in the Lower Congo region were sampled for petrographical analyses. They crop out in two well-preserved quarries (Safricas, Nsussu) and in a poorly exposed cliff section covered by dense savanna grass near the SNEL electric station. Samples for thin sectioning were collected in the Safricas quarry, SNEL electric station and Nsussu quarry (Figs 1 and 3). The facies of these UDF series were described in the field using the terminology of Eyles et al. (1983). Ten oriented samples within the UDF were collected with half-meter vertical intervals for analyses of macro- and microstructures. Thin sections were studied with a standard polarizing microscope at 10X and 25X magnification, using the microstructure and microfabric terminology of van der Meer (1987, 1993) and Menzies (2000).

The structural analysis of the thin sections is based on the discrimination of two components: (1) those with particles <25–30 µm in size are termed “plasma”, and (2) those with particles >35 µm in size, are termed “skeleton grains”, and consist of individually visible mineral or organic particles. The combinations of both plasma and skeleton grains (S-matrix) can be differentiated on the basis of brittle or ductile deformations, mixed brittle and ductile (polyphased) deformation, pore water influenced or induced structures, and plasmic fabrics (van der Meer, 1997; Menzies, 2000; van der Meer & Menzies, 2011). For example, planar features (e.g., lineations, pressure shadows) are indicative of brittle deformations, whilst the rotational structures (e.g., galaxy structures, pebbles) reveal ductile deformations. Other structures, such water escapes provide an indication of effective stress and pore water conditions of the sediment being deformed (Benn & Evans, 2010). According to Baroni & Fasano (2006), cutans, pendants, neoformed minerals and translocations are considered as “secondary features”. The plasma microfabric consists of the re-orientation of the finest (<2 mm) components caused by the application of stress during sedimentation. This microfabric may be subdivided into rotational plasmic fabrics, that are marked by the rolling of the particles and the re-orientation of the finest components at the surface of larger grains, and planar plasmic fabrics, that reflect either the pervasive or discrete failure of the sediment along shear planes (Benn & Evans, 2010). The abundance of microstructures and plasma microfabrics is quantitatively determined by their frequency under the microscope. Rare/poorly developed, common/moderately developed, and abundant/well developed are showed by one, two and three dots respectively (Table 1).

5. Facies descriptions

5.1. SNEL electric station

Macroscale description: The diamictites display ~10 m-thick discontinuous beds of unsorted and ungraded matrix-supported conglomerates (Figs 3-A and 4-A). According to the terminology of Eyles et al. (1983), these beds are massive matrix-supported diamictites (Dmm: Diamictite, matrix-supported, massive). The clasts are randomly oriented, except rare clasts aligned along the SSE-NNW directions following their long a-axis. They are lithologically heterogeneous, dominantly composed of quartzites, phyllites, gneisses, granites, with only a few carbonate rocks (Fig. 4-B). One quartzite pebble displays subparallel fractures with *in situ* recementation of the fragments. Their grain size ranges from sand to pebble. Clasts smaller than 2 cm are generally angular, while those greater than 2 cm commonly display a higher degree of roundness. No striations are observed on their surface. The matrix is composed of homogeneous pale green colored muds (Fig. 4-B). The basal and upper bed contacts are not visible.

Microscale description: Skeleton grain-size distribution ranges up than 50 µm, with an average of around 200 µm (Fig.

		Safricas quarry						SNEL station			Nsussu
		BCJ12	BCJ13	BCJ14	BCJ15	BCJ16	BCJ17	BPC21	BPC22	BPC23	BCR1
Skeleton	Average grain size (μm)	300	150	200	150	300	200	150	200	200	250
	Sorting	mod.	poorly	poorly	poorly	poorly	poorly	poorly	poorly	poorly	poorly
	Shape	<200 μm	A/SA	SA	SA	SA	SA	SA	SA	SA	A/SA
	>200 μm	SR	SR	SR	SR	SR	SR	SR	SR	SR	
Matrix	Grains	**	**
	Clays	.	**	**	**	**	**	**	**	**	.
Plasmic fabric	Skelsepic	**
	Lattisepic					
	Omnisepic
	Insepic										
	Masepic										
	Unistrial										
	Rotation	.	***	***	***	***	***	.	***	***	.
Deformation	Pressure shadow	**	.	.						.	**
	Crushed grains	.									.
	Pebble I										
	Pebble II										
	Pebble III		**
	Lineations	**	.	.	.
Water escape											
Marine	Dropstones										

Table 1. Summary of microscale soft-sediment deformation structures within the Upper Diamictite Formation. The abundance of the microstructures and plasma microfabrics is quantitatively determined by the frequency of these features observed with the microscope. Rare/poorly developed, common/moderately developed, and abundant/well developed are shown by one, two and three dots respectively. Abbreviations: A, angular; SA, subangular, SR, subrounded.

5-A; Table 1). The <200 μm grain-size fraction is subangular to angular, and the >200 μm fraction is subrounded. Quartz is dominant. Lithic fragments having magmatic (granites), metamorphic (quartzites, phyllades, gneisses) and sedimentary origins (shales, sandstones) are widely present while K-feldspars and plagioclases are rare. The distribution of skeleton grains is homogeneous, and the grains are very poorly sorted (Fig. 5-A). The matrix comprises smaller grains (<4 μm) consisting mainly of pale green colored clays. The matrix does not react with cold diluted HCl. The ratio between skeletal and plasmic grains is 1:5.

Primary voids and sedimentary structures are absent. Discrete planar shear deformations are common and show linear features with preferred fabric orientations and alignments of the skeletal grains (Fig. 5-B). Most deformations are rotational with circular alignments with or without “core stone”, galaxy structures and discrete asymmetric pressure shadows (Fig. 5-B). Clasts in grain-to-grain contacts exhibit pressure shadows marked by finer material resulting from grain crushing process. Isolated well-rounded aggregates of homogeneous material of clay or quartz grains (pebble-type III structure; van der Meer, 1993), often rimmed by circular

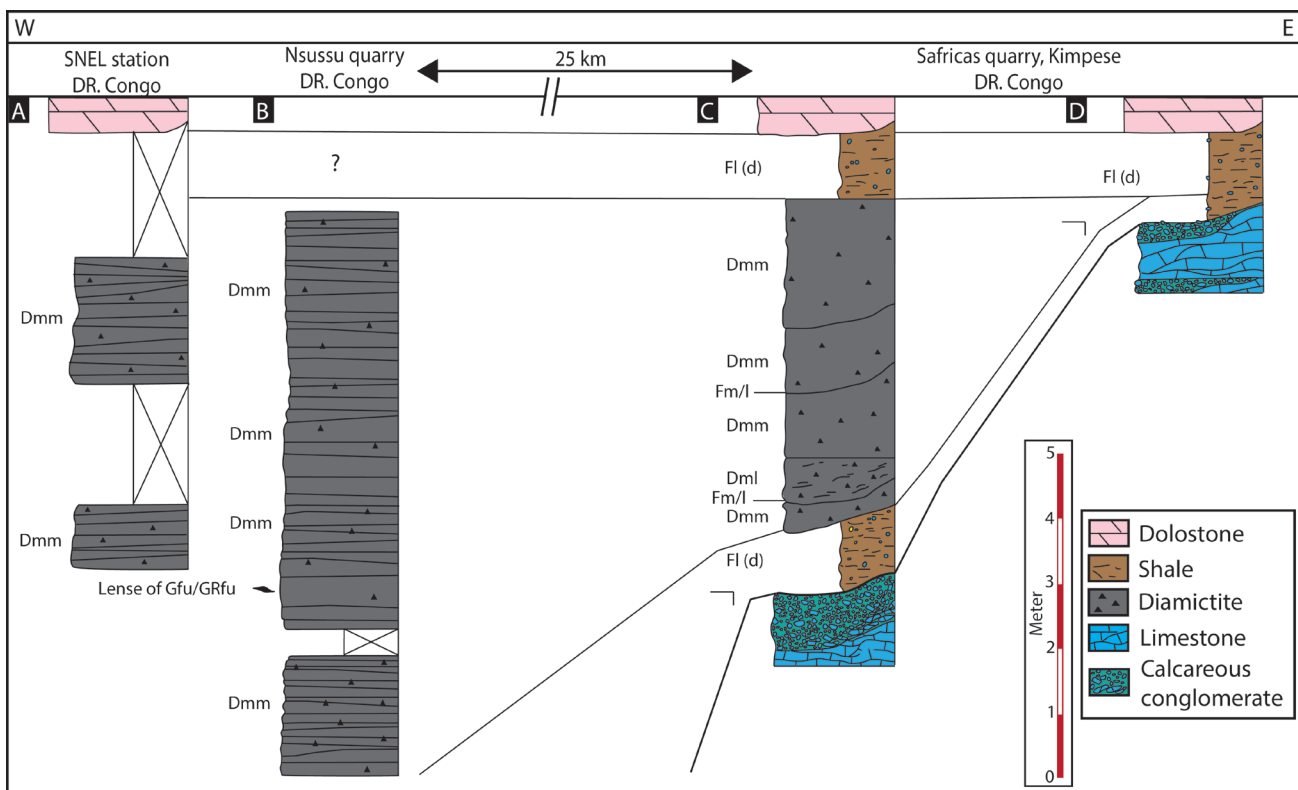


Figure 3. Detailed logged sections coupled with facies using the terminology of Eyles et al. (1983). (A) SNEL Station (S05°37.143/E014°15.638); (B) Nsussu quarry (S05°37.659/E014°14.958); (C,D) Safricas quarry (S05°34.110/E014°25.138). Terminology: Dmm: diamictite, massive; Dml: diamictite, matrix-supported, laminated; Fl(d): silts and clays, fine lamination with dropstones; Fm/l(d): silts and clays, massive or laminated; Gfu: gravels, upward-fining; GRfu: granules, upward-fining.



Figure 4. SNEL station – (A) Stack beds of unsorted and ungraded matrix-supported diamictites (Dmm) submitted to regional fracturing related to the West Congo Belt; (B) Pale green colored muddy matrix with granules and pebbles of quartzite, phyllite and gneiss.

alignments of small grains, constitute the largest clasts in size observed in thin sections. The plasmic fabric is skelsepic (Brewer, 1976), but pervasive shear lines with omniseptic plasmic fabrics are also observed (Fig. 5-B).

5.2. Nsussu quarry

Macroscale description: The diamictites exhibit ~25 m-thick continuous beds showing E-W stacking due to local deformations (Fig. 6-A). The UDF displays ~1 m-thick individual beds of poorly sorted predominantly wine-red and more exceptionally pale green massive matrix-supported diamictites (Dmm) (Figs 3-B and 6-B). The clasts

are dominantly grey-green phyllites, pale yellow quartzites, wine-red quartzophyllades and cherts with almost no dark limestones from the underlying Haut-Shiloango Subgroup. Moreover, magmatic and metamorphic rocks, including amphibolites, granites, charnockites and gneisses, are also quite abundant. The grain size of clasts ranges from sand to pebble. Clasts smaller than 2 cm are generally angular, while clasts greater than 2 cm commonly display a higher degree of roundness. None of the diamictite beds exhibits any grading. No internal structures are visible, except for several 5-10 cm-thick lenses forming a linear stone line, with upward-fining gravels and granules (Gfu + GRfu: Gravels and Granules,

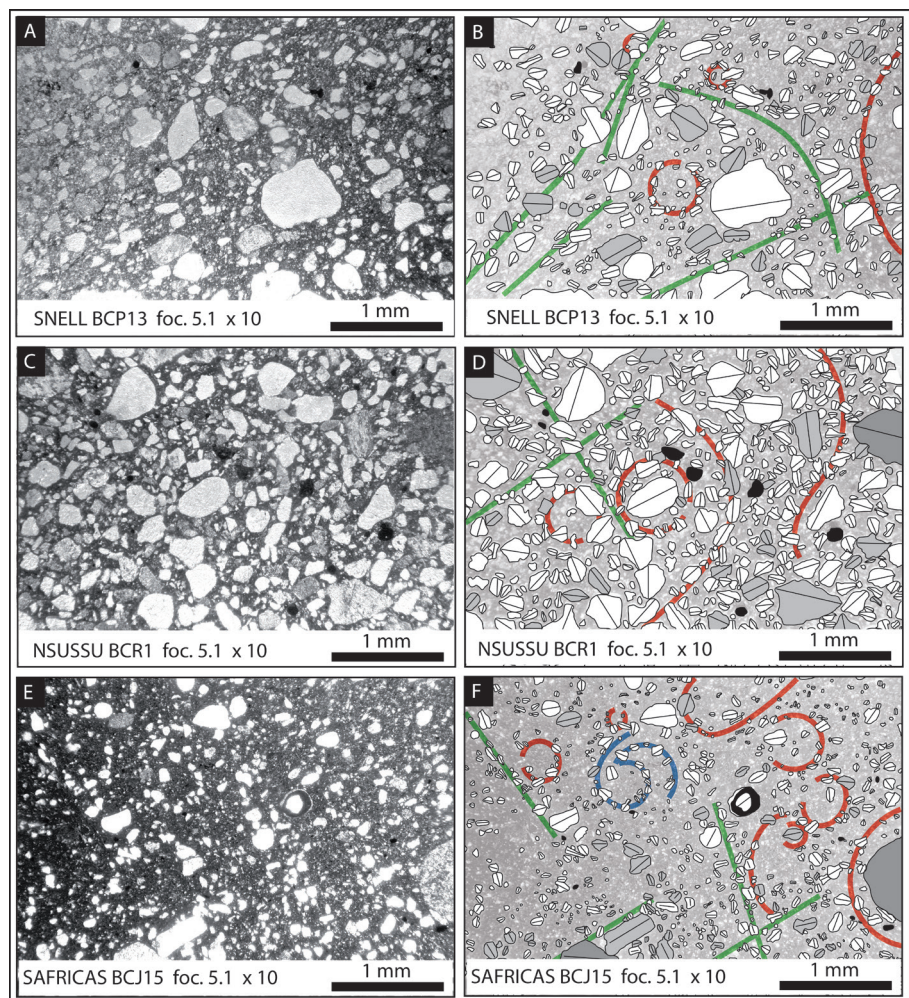


Figure 5. Paired thin-section photographs and interpretation of soft-sediment deformation structures within the Upper Diamictite Formation – (A,B) Discrete planar shear and rotational deformations in skelsepic fabrics. SNEL station, sample BP13; (C,D) Discrete planar shear deformations and strong pressure shadows in skelsepic fabrics. Nsussu quarry, sample BCR1; (E,F) Poorly sorted silty to sandy-size grain distributions in calcareous muddy matrix showing many rotational structures with circular alignments with or without galaxy structures and discrete asymmetric pressure shadows. Safricas quarry, sample BCJ15. The direction of long a-axis is indicative of planar shear and rotational structures. Planar shear structure in green, rotational structure in red, galaxy structure in blue.

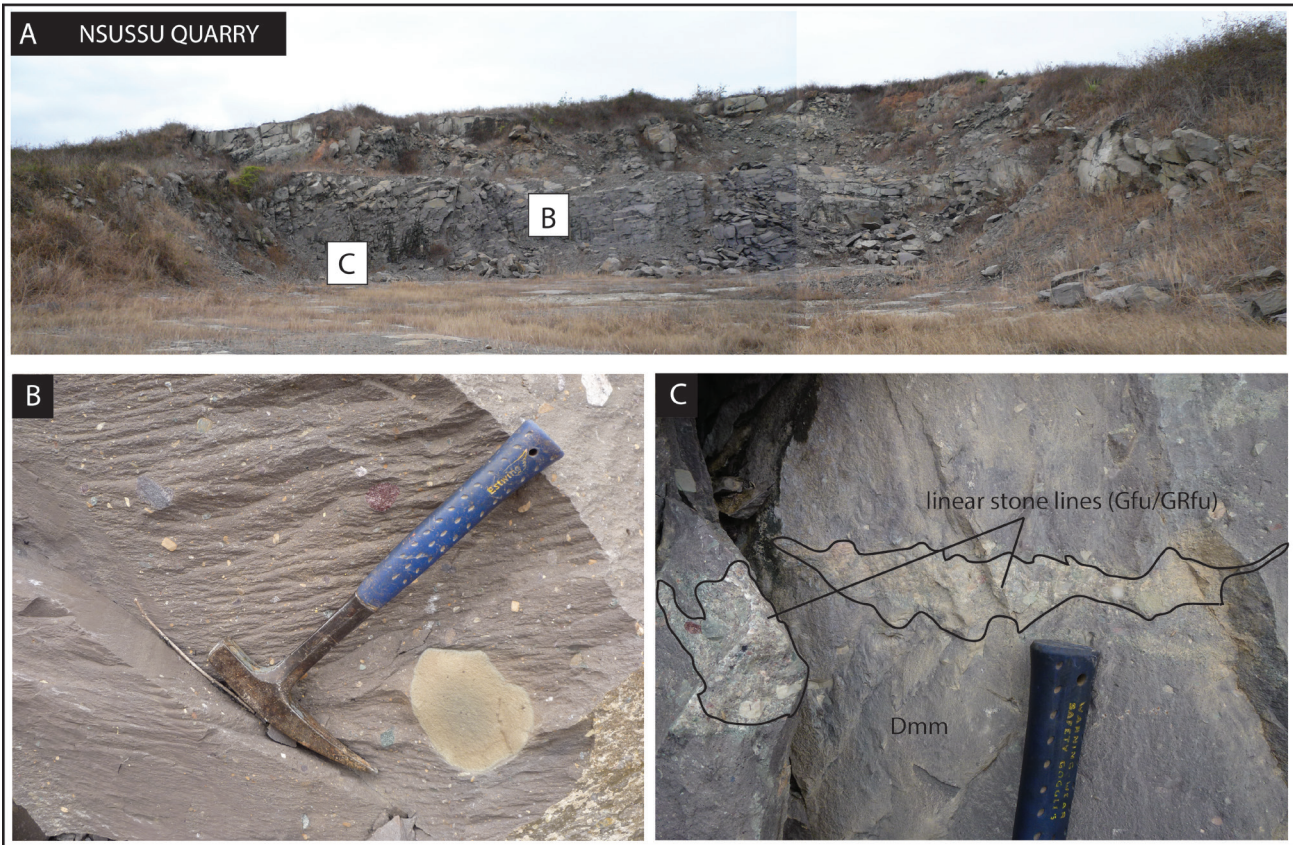


Figure 6. Nsussu quarry – (A) General view of E-W oriented outcrop with stacked beds of diamictites; (B) Wine-red massive matrix-supported diamictites (Dmm) with clasts of quartzite, wine-red quartzophyllade, chert, granite and gneiss; (C) 5-10 cm-thick lense, forming a linear stone line, with upward-finishing gravels (Gfu) and granules (GRfu) in sandy matrix within a mud-supported matrix (Dmm).

upward-finishing) in a sandy matrix (Fig. 6-C). These horizons have a loaded contact with the diamictites. The basal and upper contacts of the UDF are not observed.

Microscale description: Skeleton grain-sizes range from 20-500 μm , with an average grain size of 250 μm (Fig. 5-C; Table 1). The grain-size fractions smaller than 200 μm are subangular to angular, while those greater than 200 μm are surrounded. Quartz grains are dominant, while K-feldspars and plagioclases are rare. Lithic fragments are dominantly phyllites and quartzophyllades. The skeleton grains are poorly sorted (Fig. 5-C). The matrix does not react with cold diluted HCl. The ratio between skeletal and plasmic grains varies between 1:2 and 1:3.

Primary voids and sedimentary structures are not visible. Discrete planar shear deformations consist of microclasts arranged into linear features (Fig. 5-D). Rotational structures composed of circular alignments with or without “core stone”, are common (Fig. 5-D). Grain-to-grain contacts between clasts exhibit pressure shadows marked by finer material resulting from grain crushing processes. Plasmic fabric is principally lattic-skelsepic, where plasmic particules are preferentially oriented around skeleton grains, with randomly oriented minor diffuse arrangements of the finest components (<2 mm) (Fig. 5-D).

5.3. Safricas quarry

Macroscale description: Facies within the UDF consist of 0.5-1 m-thick massive beds of pale green colored laminated (Dml: Diamictites, matrix-supported, laminated) and massive (Dmm) matrix-supported diamictites with rounded to subrounded clasts ranging in size from silt to gravel (Figs 3-C, D and 7-A to D). Limestone-derived clasts from the underlying Haut-Shiloango Subgroup are dominant with a few phyllites, quartzites, dolerites, felsic lavas, granites and gneisses. The clasts are subangular to subrounded, with rare randomly oriented straight striations on their surface. One quartzite

pebble displays close subparallel fractures. The dominant orientation of clasts is NNW–SSE. The basal contact of the diamictite beds is slightly erosional and scoured. Beds can be traced along outcrops for some 50-100 m, appearing as lenticular channel fills, up to 5 m-thick, and include to brown colored calcareous mudstones (Figs 7-A, B). Mudstone facies show floating rounded limestones (isolated clasts) (Fl(d): Silts and clays, fine lamination with dropstones), similar in shape to glacial dropstones, dominantly composed of limestones ranging in size from sands to boulders from the underlying Haut-Shiloango Subgroup (Figs 7-A, C).

Microscale description: The grain-size fractions smaller than 200 μm are angular, while those greater than 200 μm are rounded (Fig. 5-E; Table 1). Quartz is dominant and K-feldspars and plagioclases are rare. Lithic clasts of limestones, e.g., lime mudstones and oolitic grainstones, from the underlying Haut-Shiloango Subgroup are ubiquitous, while phyllites, quartzophyllades and subordinate granites are rare. The matrix reacts with cold diluted HCl. No distinct voids were observed except vugs resulting from the chloritization and sericitization of K-feldspars and plagioclases. Microstructural fabrics are dominantly rotational with occasional galaxy-like structures and discrete asymmetric pressure shadows (Fig. 5-F). Grain-to-grain contacts exhibit pressure shadows of finer material created by grain crushing. The samples show a weakly-developed pebble type III structure (van der Meer, 1993) of *in situ* rounded pebbles with or without internal plasmic fabric (orientation of colloidal particles smaller than 20 μm based on the optical properties of aligned plasma particles) (Fig. 5-F). Pebbles without internally plasmic fabric, named “rolling ball structures” (Baroni & Fasano, 2006), are present. Samples display diffuse arrangement of the finest components (<4 μm) throughout the matrix. The plasmic fabric displays dominantly rotational plasmic fabrics (skelsepic, latticsep and omnisepic) (Fig. 5-F and Table 1). Some samples present coatings of clay around silty and sandy grains.

6. Interpretation and discussion: glacial or non-glacial in origin

6.1. Micromorphological features

Thin-section analysis highlights that the UDF is linked to soft-sediment deformations (SSD), indicative of specific sedimentological conditions during and immediately after deposition. Such deformations can be produced in a broad range of environments from volcanic to glacial as well as in subaerial and subaqueous settings (van der Meer, 1987, 1993, 1997; Menzies, 1998; Menzies & Maltman 1992; Menzies et al., 1997, 2006; Eyles & Januszczak, 2004; Evans et al., 2006). Syndepositional pervasive SSD are evidenced by the clast alignments, pervasive tectonic laminations, unidirectional folding and shears (simple shear), rotational structures, pressure shadows and water escape structures (Lachniet et al., 2001; Baroni & Fasano, 2006; Phillips, 2006). The clast alignments in the UDF are the result of remobilization of

the source sediment, which overprinted the sedimentary processes, which were active during the flow and deposition of the overriding ice or the debris flows. Pervasive tectonic laminations, unidirectional folding and water escape structures are absent in the UDF. These deformations are indicative of relatively high strain ductile deformation, facilitated by elevated pore water pressures, which succeed in the decrease of the effective stress in the sediment (Menzies, 2000; Busfield & Le Heron, 2013). Unidirectional shear is characteristic of a matrix realignment under the ductile and relatively high strain brittle deformations with fracturing and faulting, during and immediately after deposition. Shear is symptomatic of high effective stress (Maltman, 1988; Menzies et al., 2006), and is common in both subglacially deformed materials and gravity flows (van der Wateren, 1995). Rotational deformation structures are dominant in the UDF and are the product of shearing within a deforming bed (van der Meer, 1993, 1997), whereby stress is accommodated around a rotating nucleus, leading to the preferential alignment of smaller clasts at the

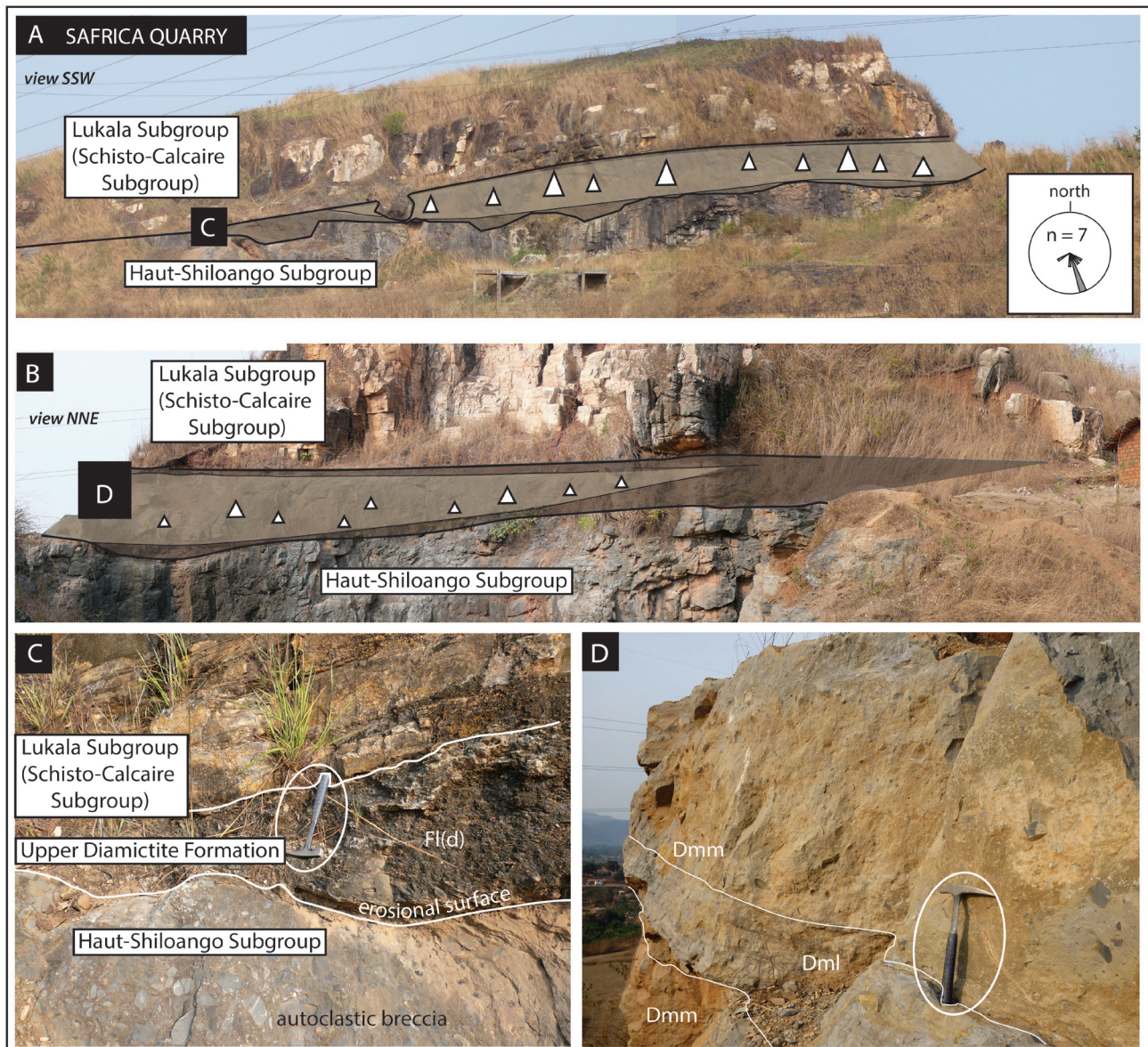


Figure 7. Safricas quarry – (A) View of the Kongo dia Kati anticline showing the lower and upper contacts of the UDF (marked with triangles) with the Haut-Shiloango and Lukala subgroups (former Schisto-Calcaire Subgroup) respectively. The basal contact is slightly erosional and beds can be traced along outcrops for some 50-100 m, appearing as lenticular channel fills inset into brown coloured calcareous mudstones (Fl(d)). Rose diagram giving a unimodal SSE paleocurrent direction of the clasts in the sediment gravity flow; (B) View of the Kongo dia Kati anticline. Calcareous mudstone facies with floating rounded lonestones (Fl(d)) present at base and the top of the diamictites; (C) Massive matrix-supported diamictites (Dmm) embedded in laminated mudstones (Fl(d)) with abundant reworked carbonate clasts from the underlying Haut-Shiloango Subgroup; (D) Basal erosional contact between the calcareous mudstones with lonestones of the Upper Diamictite Formation (Dml) and the autoclastic breccia of the upper Haut-Shiloango Subgroup (Delpomdor et al., 2014, 2016). Note the sharp upper contact between the Upper Diamictite Formation and the Lukala Subgroup.

nucleus periphery, possibly associated with re-orienting and turbulent flow in the matrix (Busfield & Le Heron, 2013). The remobilization of the matrix forms skelsepic, lattisepic and omnisepic plasmic fabrics or combinations of these, as present in the UDF. The skelsepic plasmic fabric is dominant and suggests re-orienting domains parallel to the surface of large grains (Menzies et al., 2006). The lattisepic plasmic fabric reveals a stress from two perpendicularly different directions, or that the re-orienting single high stress application event was imprinted in the narrow of former single shear plane (Menzies et al., 2006). These rotational features may be encountered in both subglacial settings (van der Meer, 1993, 1997; Menzies, 1998, 2000; Khatwa & Tulaczyk, 2001) and sediment gravity flows (Lachniet et al., 1999; Lachniet et al., 2001; Phillips, 2006). Rotational deformation structures share a common mechanical origin and are therefore not environmentally diagnostic. Additional rotational deformations are evidenced by the occurrence of soft intraclast pebbles with or without internal plasmic fabrics and pressure shadows. In the UDF, the pebbles are attributed to fine-grained pebble type-III, which is the result of reworking of the host sediment under ductile deformation. Fine-grained skeleton particles may be oriented parallel to the surface of the large skeleton grains, forming the core stone (Sitler, 1968) or a galaxy structure (van der Meer, 1993). Pressure shadow is indicative of a rotation

due to shearing (Hanmer & Passchier, 1991). Other minor deformational structures are caused by edge-to-edge grain crushing (Harker & Giegengack, 1989; Harker, 1993; Hiemstra & van der Meer, 1997; van der Meer, 1997) highlighting a cataclastic flow (Hiemstra & van der Meer, 1997; Menzies et al., 2006).

The combination of microscale SSD structures in the UDF points to an environment with relatively high strain rates in absence of pore water pressures. These deformational features reveal that the UDF has dominantly been subject to ductile flows and deformations, as evidenced by the rotational structures. Our SSD observations within the UDF suggest that these deformational structures share mechanical features related common to both sediment gravity flows and subglacial deposits. Therefore, they are not diagnostic of the depositional environment.

6.2. Macroscale features

As only micromorphological features do not unambiguously discriminate the depositional environment, macroscale observations have also to be taken into account. Diagnostic subglacial settings develop under high strain pore water pressure by high overburden pressure of ice and basal meltwater supply. They include flow noses, tiles structures, glaciotectionic laminations, unidirectional foldings, clast

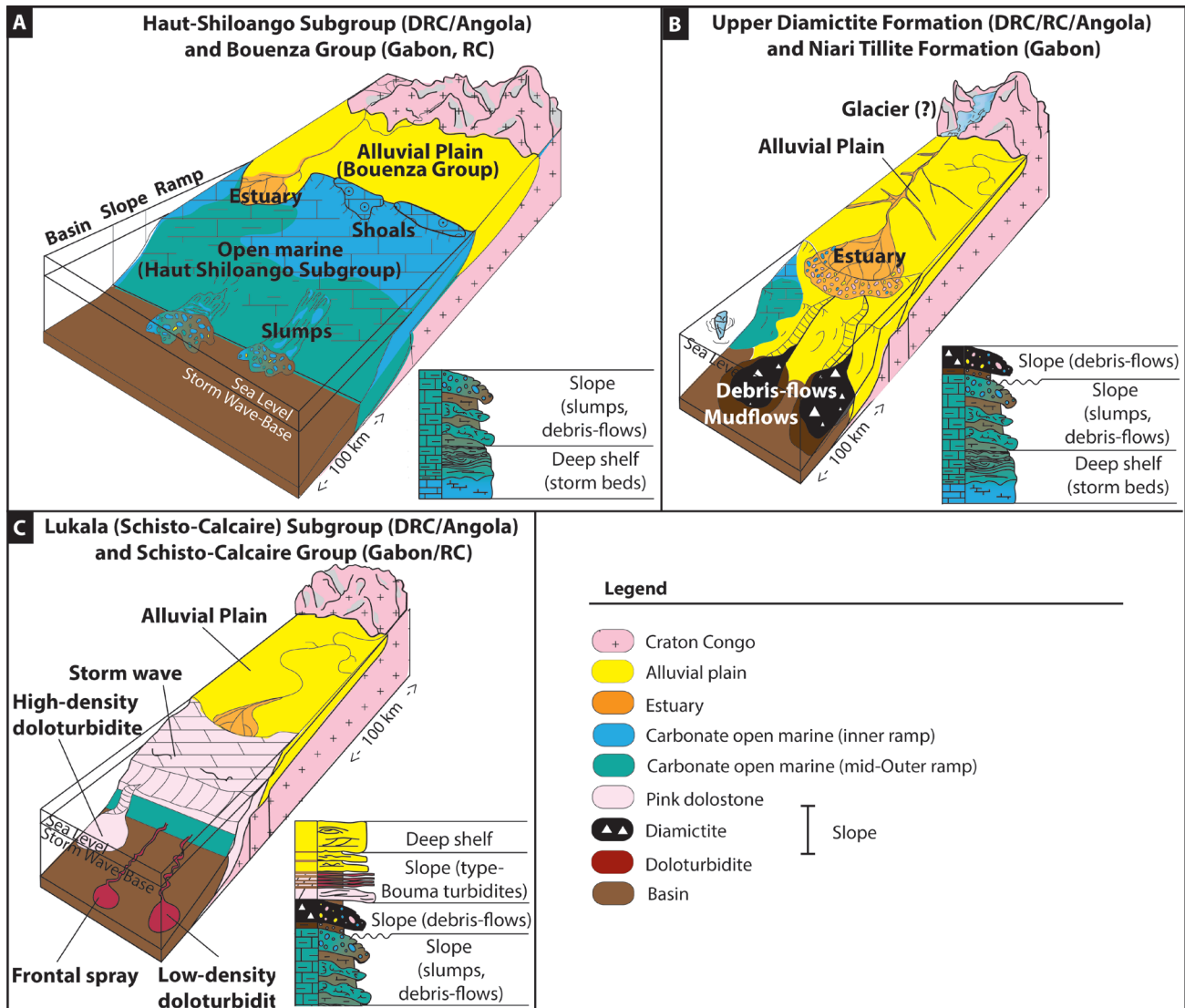


Figure 8. Reconstruction of depositional environments of the West Congolian ramp. The idealized 3D model illustrates the spatial and vertical distribution of deep marine and alluvial fan system including steepened ramp of the Haut-Shiloango Subgroup, glacially-influenced sediment gravity flows of the Upper Diamictite Formation, and deep-water turbidites at the base of the Lukala Subgroup (former Schisto-Calcaire Subgroup) in the Democratic Republic of Congo (after Delpomdor et al., 2016). No vertical scale intended.

dispersion tails and fracturing at the base of the diamictite. All these features are absent in the studied sections. Derivation of the UDF by subglacial deposition is therefore rejected. Additional evidences of non-subglacial deposits are the absence of diagnostic features typical of direct ice-contact deposits (i.e., tills) such as boulder pavements, associated meltwater deposits, and common presence of striated and glacially-shaped clasts. Striated and dislodged pebbles of quartzites were found to the north of the Sansikwa massif (Cahen, 1963), and the latter rocks are therefore interpreted as the result of interparticulate shocks which are formed by the gravitational flowage of sediment-water mixtures. Less than 1% of clasts are striated, and no striations are present on the fine-grained lithologies such as the limestones, phyllites and dolerites (Tack, L., Royal Museum for Central Africa, pers. comm.). Striation is encountered in both subglacial settings and sediment gravity flows by friction during an active flow. Their exceptional occurrence – particularly in the proximal facies along the Congo craton in Gabon – suggests that the UDF does not result from a continental glacial accumulation (Delpomdor et al., 2016). At the Safricas quarry, a shear zone at the base of the Dml facies exhibits a high stress accompanied by an upward decrease in strain intensity, as evidenced by the deposition of Dmm facies. Such deformation structures are characteristic of sediment gravity flow deposits, where the water pressure is in excess of the hydrostatic pressure and thus reduces the shear strength of this material, which may even be liquefied (Lachniet et al., 2001). Rare load structures with normal grading including gravels and granules (Gfu + GRfu) in a sandy matrix are indicative of small plug-flow channels. However, no evidence of vertical to subvertical water escape structures has been encountered, thus pointing to sediment gravity flow deposition (Bertran et al., 1995; Bertran & Texier, 1999; Lachniet et al., 2001; Menzies & Zaniewski, 2003; Phillips, 2006). Gravity flow deposits can produce erosional features, such as scours at the contact with the Haut-Shiloango carbonates, in the form of broad channels. The calcareous mudstones (Fl) embedding the diamictite are interpreted as contemporaneous pelagic clays expelled from the tops of the muddy gravity flows or as deposit of muddy gravity flows with floating clasts as evidenced by the lonestones. The emplacement of the lonestones in the mass flow dominated successions is related to the transport of clasts having settled down from subsequent hyperconcentrated flows (Mutti, 1992). The absence of clear evidence of dropstones, of till pellets and conglomeratic lenses (see Drewry, 1986) is at variance with deposition of ice-rafted debris. Subaqueous mass flows as slumps, debris flows and turbidites can be indicative of glacial affinity, especially during periods of rapid retreat of ice and abundant sediment input or *via* the subglacial flow in the edge of slope (Van Vliet-Lanoë, 2005), but have in no way to be necessarily linked to a cold climate.

In view of our micro- and macroscale observations the UDF is therefore interpreted as the result of subaqueous gravity flow deposits (debrites) because of (1) the combination of ductile deformation, brittle deformation and grain-to-grain compression, considered as evidence of high strain rates and local high stress conditions, typical of mass flow in a subaqueous environment; (2) the contemporaneous pelagic clays expelled from the tops of the muddy gravity flows, and (3) the absence of diagnostic features typical of direct ice-contact deposits (i.e., tills) such as glaciotectionic deformations, boulder pavements, associated meltwater deposits, common striated and glacially-shaped clasts.

7. A model of subaqueous sediment gravity flow for the UDF

Deposition of the UDF is thus here interpreted as subaqueous sediment gravity flows (debrites), with only limited glacial influence. It is linked to deep-water submarine to alluvial fan systems along the unstable margins of a carbonate ramp, perhaps at the foot of the basin slope (Delpomdor et al., 2016) (Fig. 8). This is in line with uplift of the Chaillu massif of Gabon and the Republic of Congo (located to the NW

of the UDF) acting as source region for most of the UDF clasts (Wagner & Wilhelm, 1971), including also our observed charnockites and felsic rocks. Gravity driven sedimentation was followed by the progradation of an alluvial fan and a deep-water submarine fan system towards the south and the west, i.e., from what is now northern Angola. Subaqueous gravity flow deposits were frequent especially during periods of rapid marine transgression in the basin (Delpomdor et al., 2016). The envisaged deep-water environment already preceded and followed UDF deposition. Indeed, it is recorded in respectively the upper part of the Haut-Shiloango Subgroup and lower part of the Lukala Subgroup (Delpomdor et al., 2016). Debris flow deposits developing broad channels – and in general the envisaged deep-water sedimentary environment – were probably triggered by over steepening and/or tectonic shock events. The latter can tentatively be related to the extensional tectonic movements associated with the 660 Ma oceanic spreading in the central-southern Macaúbas Basin (now located in present-day Brazil) preceding the onset of the 630 Ma pre-collisional magmatic arc of the Araçuaí-West Congo Orogen (Pedrosa-Soares et al., 2011). In line with the E1-E6 terminology of Pedrosa-Soares & Alkmin (2011) to describe successive rifting events preceding the AWCO, we suggest to name our new evidence of extensional tectonic movement on the African side as the “E7” event (660–630 Ma). No anomalous or abrupt climatic or eustatic events such as proposed by the Snowball Earth ice age model are thus recorded in the UDF. On the contrary, our envisaged deep-water environment reflects an overriding, long-term and diachronous tectonic control on sedimentation along the western margin of the Congo Craton during regional extension induced by the break-up of the Rodinia supercontinent.

8. Conclusions

The Upper Diamictite Formation (UDF) of the West Congo Supergroup has hitherto often been considered as a record of a glacial-interglacial transition related to the Snowball Earth-type Marinoan event because it was considered to be a true tillite. Our paper shows that the UDF corresponds to subaqueous sediment gravity flows deposited along the margins of a basin. Any substantial glacial influence is not readily identifiable. The deep-water sedimentary facies reported here primarily record mass flow processes. No catastrophic climatic events (i.e., Snowball Earth) can thus be identified in the UDF. On the contrary, the deep-water facies – not only recorded in the UDF (this paper) but also in respectively the underlying upper part of the Haut-Shiloango Subgroup and lower part of the Lukala Subgroup – reflect a strong regional tectonic control. Extensional movements preceding the Araçuaí-West Congo Orogen (660–630 Ma) are suggested to control long-term and diachronous sedimentation along the western margin of the Congo Craton. In line with the E1-E6 terminology of Pedrosa-Soares & Alkmin (2011), we suggest to name this new evidence of rifting event on the African side the “E7” event (660–630 Ma).

9. Acknowledgements

The authors wish to thank the Centre de Recherches Géologiques et Minières (CRGM), Kinshasa, Democratic Republic of Congo, for the organization of a fieldtrip in the Lower Congo region as well as the Royal Museum for Central Africa (RMCA), Tervuren, Belgium, for access to its facilities. We acknowledge Olivier Caron, Scott Elrick for the helpful comments and discussions on the manuscript. We are grateful to Kristen Kennedy and Daniel Baudet for their careful edits that significantly improved the manuscript.

10. References

- Affaton, P., Kalsbeek, F., Boudzoumou, F., Trompette, R., Thrane, K. & Frei, R., 2016. The Pan-African West Congo belt in the Republic of Congo (Congo Brazzaville): Stratigraphy of the Mayombe and West Congo Supergroups studied by detrital zircon geochronology. *Precambrian Research*, 272, 185–202.

- Baroni, C. & Fasano, F., 2006. Micromorphological evidence of warm-based glacier deposition from the Ricker Hills Tillite (Victoria Land, Antarctica). *Quaternary Science Reviews*, 25, 976–992.
- Baudet, D., Fernandez, M., Kant-Kabalu, F. & Laghmouch, M., 2013. Carte géologique de la République Démocratique du Congo au 1/500 000° - Province du Bas-Congo. Musée royal de l'Afrique centrale, Tervuren, Belgique & Centre de Recherches Géologiques et Minières, Kinshasa, RD Congo, avec une notice explicative de 50 p.
- Benn, D.I. & Evans, D.J.A., 2010. *Glaciers and Glaciation*. 2nd ed. Hodder Arnold Publication, Oxon, 816 p.
- Bertran, P. & Texier, J.-P., 1999. Facies and microfacies of slope deposits. *Catena*, 35, 99–121.
- Bertran, P., Francou, B. & Texier, J.-P., 1995. Stratified slope deposits: the stone-banked sheets and lobes model. In Slaymaker, O. (ed.), *Steepland geomorphology*. Wiley, London, 147–169.
- Brewer, R., 1976. *Fabric and Mineral Analysis of Soils*. Krieger, Huntington, 482 p.
- Busfield, M.E. & Le Heron, D.P., 2013. Glacitectonic deformation in the Chuos Formation of northern Namibia: implications for Neoproterozoic ice dynamics. *Proceedings of the Geologists' Association*, 124/5, 778–789.
- Cahen, L., 1948. Les formations anciennes, antérieures à la Tillite du Bas-Congo (Le groupe des Monts de Cristal). *Bulletin de la Société belge de Géologie, de Paléontologie et d'Hydrologie* 57/1, 77–148.
- Cahen, L., 1950. Le Calcaire de Sekelolo, le Complexe tillitique et la Dolomie rose C1 dans l'Anticlinal de Congo dia Kati (Bas-Congo). *Annales du Musée royal du Congo belge, Tervuren*, in 8°, Sciences Géologiques, 7, 55 p.
- Cahen, L., 1963. Glaciations anciennes et dérive des continents. *Annales de la Société Géologique de Belgique*, 86/1, B19–B83.
- Cahen, L., 1978. La stratigraphie et la tectonique du Supergroupe Ouest-Congolien dans les zones médiane et externe de l'orogène Ouest-Congolien (Pan-Africain) au Bas-Zaïre et dans les régions voisines. *Annales du Musée royal de l'Afrique Centrale, Tervuren*, in 8°, Sciences Géologiques, 83, 150 p.
- Cahen, L. & Lepage, J., 1976. Les mixtites du Bas-Zaïre: mise au point intérimaire. Musée royal de l'Afrique Centrale, Tervuren (Belgique), Département de Géologie et de Minéralogie, Rapport annuel 1975, 33–57.
- Dadet, P., 1969. Notice explicative de la carte géologique de la République du Congo-Brazzaville au 1/500 000. *Mémoires du Bureau de Recherches Géologiques et Minières*, 70, 103 p.
- Delpomdor, F., Kant, F. & Préat, A., 2014. Neoproterozoic Uppermost Haut-Shiloango Subgroup (West Congolian Supergroup, Democratic Republic of Congo): Misinterpreted stromatolites and implications for sea-level fluctuations before the onset of the Marinoan glaciation. *Journal of African Earth Sciences*, 90, 49–63.
- Delpomdor, F., Eyles, N., Tack, L. & Préat, A., 2016. Pre- and post-Marinoan carbonate facies of the Democratic Republic of Congo: glacially- or tectonically-influenced deep-water sediments. *Palaeogeography, Palaeoclimatology, Palaeoecology*, 457, 144–157.
- De Paepe, P., Hertogen, J. & Tack, L., 1975. Mise en évidence de laves en coussin dans les faciès volcaniques basiques du massif de Kimbundu (Bas-Zaïre) et implications pour le magmatisme ouest-congolien. *Annales de la Société Géologique de Belgique*, 98, 251–270.
- Drewry, D.J., 1986. *Glacial Geologic Processes*. Edward Arnold, London, 276 p.
- Evans, D.J.A., Phillips, E.R., Hiemstra, J.F. & Auton, C.A., 2006. Subglacial till: formation, sedimentary characteristics and classification. *Earth Science Reviews*, 78, 115–176.
- Eyles, N. & Januszczak, N., 2004. 'Zipper-rift': a tectonic model for Neoproterozoic glaciations during the breakup of Rodinia after 750 Ma. *Earth Science Reviews*, 65, 1–73.
- Eyles, N. & Januszczak, N., 2007. Syntectonic subaqueous mass flows of the Neoproterozoic Otavi Group, Namibia: where is the evidence of global glaciation? *Basin Research*, 19, 179–198.
- Eyles, N., Eyles, C.H. & Miall, A.D., 1983. Lithofacies types and vertical profile models: an alternative approach to the description and environmental interpretation of glacial diamicton and diamictonite sequences. *Sedimentology*, 30, 393–410.
- Frimmel, H.E., Tack, L., Basei, M.S., Nutman, A.P. & Boven, A., 2006. Provenance and chemostratigraphy of the Neoproterozoic West Congolian Group in the Democratic Republic of Congo. *Journal of African Earth Sciences*, 46, 221–239.
- Hanmer, S. & Passchier, C., 1991. Shear-sense indicators: a review. *Geological Survey of Canada Paper* 90-17, vi + 72 p.
- Harker, R.I., 1993. Fracture patterns in clasts of diamictonites (? tillites). *Journal of the Geological Society*, London, 150, 251–254.
- Harker, R.I. & Giegengack, R., 1989. Brecciation of clasts in diamictonites of the Gowganda Formation, Ontario, Canada. *Geology*, 17, 123–126.
- Harland, W.B., 1964. Critical evidence for a great Infra-Cambrian Glaciation. *Geologische Rundschau*, 54, 45–61.
- Harland, W.B. & Bidgood, D.E.T., 1959. Palaeomagnetism in some Norwegian sparagmites and the late pre-Cambrian ice age. *Nature*, 184, 1860–1862.
- Hiemstra, J.F. & van der Meer, J.J.M., 1997. Pore-water controlled grain fracturing as an indicator for subglacial shearing in tills. *Journal of Glaciology*, 43, 446–454.
- Hoffman, P.F. & Schrag, D.P., 2002. The snowball Earth hypothesis: testing the limits of global change. *Terra Nova*, 14, 129–155.
- Hoffman, P.F., Kaufman, A.J., Halverson, G.P. & Schrag, D.P., 1998. A Neoproterozoic Snowball Earth. *Science*, 281, 1342–1346.
- Kampanzu, A.B., Kapenda, D. & Manteka, B., 1991. Basic magmatism and geotectonic evolution of the Pan African belt in central Africa: evidence from the Katangan and West Congolian segments. *Tectonophysics*, 190, 363–371.
- Kant-Kabalu, F., Kadja-Wongudi, G., Mujinga-Mulemba, E., Nseka-Mbemba, P., Phambu-Landu, J., Kanda-Nkula, V., Baudet, D., Dewaele, S., Eekelers, K., Fernandez, M., Laghmouch, M., Theunissen, K. & Tack, L., 2016. New 1/500.000 scale GIS-based geological and mineral resources maps for Bas-Congo province (DRC) with an updated lithostratigraphy of the Neoproterozoic West Congo Supergroup. 5th International Geologica Belgica 2016 Congress, 26-29 January 2016, University of Mons, Mons, Belgium. Abstract Book, 42–43.
- Khatwa, A. & Tulaczyk, S., 2001. Microstructural interpretations of modern and Pleistocene subglacially deformed sediments: the relative role of parent material and subglacial process. *Journal of Quaternary Science*, 16, 507–517.
- Kirschvink, J.L., 1992. Late Proterozoic low-latitude global glaciation: the Snowball Earth. In Schopf, J.W. & Klein, C. (eds), *The Proterozoic Biosphere: a Multidisciplinary Study*. Cambridge University Press, Cambridge, 51–52.
- Kröner, A. & Correia, H., 1973. Further evidence for glaciogenic origin of late Precambrian mixtites in Angola. *Nature, Physical Sciences*, 246, 115–117.
- Lachniet, M.S., Strasser, J.C., Larson, D.E., Evenson, E.B. & Alley, R.D., 1999. Microstructures of glaciogenic sediment-flow deposits, Matanuska Glacier, Alaska. In Mickelson, D.M. & Attig, J.W. (eds), *Glacial Processes Past and Present*. Geological Society of America, Boulder, Colorado, Special Paper 337, 45–57.
- Lachniet, M.S., Larson, D.E., Lawson, E.B., Evenson, E.B. & Alley, R.D., 2001. Microstructures of sediment flow deposits and subglacial sediments: a comparison. *Boreas*, 30, 254–264.
- Lepage, J., 1951. Données nouvelles sur la stratigraphie des territoires anciens du Bas-Congo. *Bulletin de la Société belge de Géologie, de Paléontologie et d'Hydrologie*, 60/2, 169–189.
- Lepage, J., 1973. Carte géologique à l'échelle de 1/200.000. Notice explicative de la feuille Ngungu (degré carré S6/14 = SB 33.9). République du Zaïre, Ministère des Mines, Direction du Service Géologique, 66 p.
- Maltman, A.J., 1988. The importance of shear zones in naturally deformed wet sediments. *Tectonophysics*, 145, 163–175.
- Menzies, J., 1998. Microstructures within subglacial diamictons. In Kostorzewski A. (ed), *Relief and Deposits of Present-day and Pleistocene Glaciation of the Northern Hemisphere – selected problems*. Adam Michiewicz University Press, Poznan, Geography Series, 58, 153–156.
- Menzies, J., 2000. Micromorphological analyses of microfabrics and microstructures indicative of deformation processes in glacial sediments. In Maltman, A.J., Hubbard, B. & Hambrey, M.J. (eds), *Deformation of Glacial Materials*. Geological Society, London, Special Publications, 176, 245–257.
- Menzies, J. & Maltman, A.J., 1992. Microstructures in diamictons—evidence of subglacial bed conditions. *Geomorphology*, 6/1, 27–40.
- Menzies, J. & Zaniewski, K., 2003. Microstructures within a modern debris flow deposit derived from Quaternary glacial diamicton—a comparative micromorphological study. *Sedimentary Geology*, 157, 31–48.
- Menzies, J., Zaniewski, K. & Dreger, D., 1997. Evidence, from microstructures, of deformable bed conditions within drumlins, Chimney bluffs, New York State. *Sedimentary Geology*, 111, 161–175.
- Menzies, J., van der Meer, J.J.M. & Rose, J., 2006. Till—as a glacial “tectomict”, its internal architecture, and the development of a “typing” method for till differentiation. *Geomorphology*, 75, 172–200.
- Muanza-Kant, P., Mpiana, Ch., Kanda-Nkula, V., Tack, L., Baudet, D., Archibald, D.B. & Glorie, S., 2016. The Lower Diamictonite Formation of the Cataractes Group, West Congo Supergroup (Bas-Congo, DRC): a 700 Ma marker of extensional episodic activity during breakup of Columbia. 5th International Geologica Belgica 2016 Congress, 26-29 January 2016, University of Mons, Mons, Belgium. Abstract Book, p. 57.

- Mutti, E., 1992. Turbidite Sandstones. Special Publication Agip, Milan, 275 p.
- Pedrosa-Soares, A. C. & Alkmin, 2011. How many rifting events preceded the development of the Araçuaí-West Congo orogen? *Geonomos*, 19/2, 244–251.
- Pedrosa-Soares, A. C., Alkmin, F., Tack, L., Noce, C., Babinski, M., Silva, L. & Martins-Neto, M., 2008. Similarities and differences between the Brazilian and African counterparts of the Neoproterozoic Araçuaí-West Congo Orogen. In: Pankhurst, J., Trouw, R., Brito-Neves, B., De Wit, M. (eds), *West Gondwana: Pre-Cenozoic Correlations across the South Atlantic Region*. Geological Society, London, Special Publications, 294, 153–172.
- Pedrosa-Soares, A., C., de Campos, C., Noce, C., Silva, L., Novo, T., Roncato, J., Medeiros, S., Castaneda, C., Queiroga, G., Dantas, E., Dussin, I. & Alkmin, F., 2011. Late Neoproterozoic-Cambrian granitic magmatism in the Araçuaí orogen (Brazil), the Eastern Brazilian pegmatite Province and related mineral sources. In Sial, A., Bettencourt, J., de Campos, C. & Ferreira, V. (eds), *Granite-Related Ore Deposits*. Geological Society, London, Special Publications, 350, 25–51.
- Phillips, E., 2006. Micromorphology of a debris flow deposit: evidence of basal shearing, hydrofracturing, liquefaction and rotational deformation during emplacement. *Quaternary Science Reviews*, 25, 720–738.
- Poidevin, J.-L., 2007. Stratigraphie isotopique du strontium et datation des formations carbonatées et glaciogéniques néoproterozoïques du Nord et de l'Ouest du craton du Congo. *Comptes Rendus Geoscience*, 339, 259–273.
- Sitler, R.F. 1968. Glacial till in oriented thin section. XXIII International Geological Congress, Prague, 8, 283–295.
- Schermerhorn, L.J.G., 1981. Late Precambrian tilloids of northwestern Angola. In Hambrey, M.J. & Harland, W.B. (eds), *Earth's Pre-Pleistocene Glacial Record*. Cambridge University Press, Cambridge, 158–161.
- Schermerhorn, L.J.G. & Stanton, W.I., 1963. Tilloids in the West Congo geosyncline. *Quarterly Journal of the Geological Society of London*, 119, 201–241.
- Straathof, G.B., 2011. Neoproterozoic low latitude glaciations: An African perspective. Unpublished PhD thesis. University of Edinburgh, 283 p.
- Tack, L., Wingate, M.T.D., Liégeois, J.-P., Fernandez-Alonzo, M. & Deblond, A., 2001. Early Neoproterozoic magmatism (1000–910 Ma) of the Zadinian and Mayumbian groups (Bas-Congo), onset of Rodinia rifting at the western edge of the Congo Craton. *Precambrian Research*, 110, 277–306.
- Tack, L., Fernandez-Alonso, M., Kanda Nkula, V., Mpoyi, J., Delvaux, D., Trefois, Ph. & Baudet, D., 2006. Neoproterozoic diamictites around the Congo River Basin: a critical reappraisal of their origin. 21th Colloquium African Geology (CAG21), Maputo (Mozambique), 03-05.07.2006, Abstract book, 152–154.
- Tack, L., Theunissen, K., Delvaux, D., Everaerts, M., Fernandez-Alonso, M. & Baudet, D., 2016. The West Congo Belt of Bas-Congo (DRC) revisited: a patchwork of individual tectono-metamorphic domains as a result of South Atlantic Ocean opening. 5th International Geologica Belgica 2016 Congress, 26–29 January 2016, University of Mons, Mons, Belgium. Abstract Book, p. 58.
- Thiéblemont, D., Castaing, C., Billa, M., Bouton, A. & Prétat, A., 2009a. Notice explicative de la carte géologique et des ressources minérales de la République Gabonaise à 1/1 000 000. Programme Sysmin 8 ACP GA 017, Ministère des Mines, du Pétrole, des Hydrocarbures. Direction Générale des Mines et de la Géologie, Libreville, 384 p.
- Thiéblemont D., Prian J.P., Goujou J.C., Boulingui B., Ekogha H., Kassadou A.B., Simo Ndounze S., Walemba A., Prétat A., Theunissen K., Cocherie A. & Guerrot C., 2009b. Timing and characteristics of Neoproterozoic magmatism in SW-Gabon. First geochronological and geochemical data on the West Congolian orogen in Gabon SYSMIN project, Gabon 2005-2009. 23th Colloquium African Geology (CAG23), Johannesburg (South Africa), January 2009, Abstract book and poster.
- van der Meer, J.J.M., 1987. Micromorphology of glacial sediments as a tool in distinguishing genetic varieties of till. *Geological Survey of Finland, Special Paper*, 3, 77–89.
- van der Meer, J.J.M., 1993. Microscopic evidence of subglacial deformation. *Quaternary Science Reviews*, 12, 553–587.
- van der Meer, J.J.M., 1997. Subglacial processes revealed by the microscope: particle and aggregate mobility in till. *Quaternary Science Reviews*, 16, 827–831.
- van der Meer, J.J.M. & Menzies, J., 2011. The micromorphology of unconsolidated sediments. *Sedimentary Geology*, 238, 213–232.
- van der Wateren, F.M., 1995. Structural geology and sedimentology of push moraines. *Mededelingen Rijks Geologische Dienst*, 54, 168 p.
- Van Vliet-Lanoë, B., 2005. *La planète des glaces*. Vuibert, Paris, 470 p.
- Vellutini, P. & Vicat, J.-P., 1983. Sur l'origine des formations conglomératiques de base du géosynclinal Ouest-Congolien (Gabon, Congo, Zaïre, Angola). *Precambrian Research*, 23, 81–101.
- Wagner, A. & Wilhelm, E., 1971. Pétrographie et statistique des galets des "Tillites" et contribution à l'étude stratigraphique de la série de la Louila dans la région du Kouilou-Niari (Congo-Brazzaville). *Bulletin du Bureau de Recherches Géologiques et Minières (deuxième série), Section IV, n° 1*, 47–57.